Journal of Asian Earth Sciences 158 (2018) 140–152

Contents lists available at ScienceDirect

Journal of Asian Earth Sciences

journal homepage: www.elsevier.com/locate/jseaes

Full length article

Late quaternary out-of-sequence deformation in the innermost Kangra Reentrant, NW Himalaya of India: Seismic potential appraisal from ^{10}Be dated fluvial terraces

J. Cortés-Aranda[a,*], R. Vassallo[b], H. Jomard[c], L. Pousse-Beltrán[b], L. Astudillo[a], J.-L. Mugnier[b], F. Jouanne[b], M. Malik[d], J. Carcaillet[b]

[a] Departamento Ciencias de la Tierra, Universidad de Concepción, Víctor Lamas 1290, Concepción, Chile
[b] Université Savoie Mont Blanc, Université Grenoble Alpes, CNRS, IRD, IFSTTAR, ISTerre, 38000 Grenoble, France
[c] Institut de Radioprotection et de Sûreté Nucléaire (IRSN), 31, avenue de la Division Leclerc, 92260 Fontenay-aux-Roses, France
[d] Department of Geology, University of Jammu, Gujarbasti, Jammu, Jammu and Kashmir 180006, India

ARTICLE INFO

Keywords:
Out-of-sequence deformation
Kangra Reentrant
Palampur Thrust
^{10}Be exposure dating
Seismic hazard

ABSTRACT

The Kangra Reentrant is a convex-to-the-northeast U-shaped structure in the NW Himalaya, where the Sub-Himalayan fold-and-thrust belt is ~90 km wide. This region has not been struck by large earthquakes since the 1905 Mw 7.8 Kangra Earthquake. Out-of-sequence deformation has been reported at the millennial timescale along intracrustal thrusts within this reentrant, such as the Jawalamukhi Thrust. Up to now, the occurrence of out-of-sequence deformation along inner thrusts within the Kangra Reentrant, during the Late Quaternary, has not yet been addressed. In this study, the results of a neotectonic survey undertaken in this reentrant are presented; the studied zone is located between the Beas and the Neogad rivers, and encompasses from the Jawalamukhi Thrust to the Main Boundary Thrust. Two terraces that are deformed by branches of the Medlicott-Wadia Thrust, locally named the Palampur Thrust, are identified; this is evidenced in the field by metric-scale fault scarps. By using ^{10}Be dating, the ages of these terraces were constrained to ca. 7.5 and ca. 6.2 ka. This is clear evidence of the Late Quaternary out-of-sequence deformation in the innermost part of this reentrant, implying that strain is distributed along all the arc-orthogonal extent of the local fold and thrust belt over this timespan. A cumulative slip rate of ca. 1 mm/yr along the studied thrusts, which represents 10% of the bulk-strain accommodated by the whole reentrant for this timespan, is calculated. In spite of the marginal appearance of this figure, this deformation rate is attributed to $7 < Mw < 8$ earthquakes triggered along the brittle/ductile zone of Main Himalayan Thrust and emerging at the surface along crustal ramps, such as those represented by the Palampur Thrust in the study area. Earthquakes of this magnitude may severely impact the Kangra District, which currently hosts 1.5 million people.

1. Introduction

Since the late 1990, researchers devoted to the Himalayan neotectonics have addressed how thrusts between the Main Boundary Thrust (MBT; e.g. (Mugnier et al., 1994)) and the Main Frontal Thrust (MFT; e.g. Wesnousky et al., 1999) – the two intracrustal faults limiting the Sub-Himalayan domain (Fig. 1) – have accommodated Late Quaternary deformation induced by the India-Eurasia collision. Past studies indicate that, during this timespan, deformation within the Sub-Himalayan fold and thrust belt is mostly accommodated by the MFT (e.g. Burgess et al., 2012; Lavé and Avouac, 2000). This signifies that, within this belt, deformation has mainly evolved according to an in-sequence pattern during the Late Quaternary. Authors like Mugnier et al. (2005), Thakur et al. (2010), Dey et al. (2016) and Devi et al. (2011), whose results have been discussed by Mukherjee (2015), propose that out-of-sequence deformation in this tectonic domain is, although existent, insignificant throughout this time interval. However, other studies conducted along the Himalaya have reported the occurrence of significant out-of-sequence deformation at the historical and millennial timescales. For instance, Wobus et al. (2006) detail an active thrust fault in Central Nepal, located ~100 km northward of the MFT, enhancing millennial scale erosion rates. Furthermore, Murphy et al. (2014) identified a 63 km long rupture along the Western Nepal Fault System, in Western Nepal, whose causative events may have occurred

* Corresponding author.
E-mail address: joacortes@udec.cl (J. Cortés-Aranda).

https://doi.org/10.1016/j.jseaes.2018.01.027
Received 19 May 2017; Received in revised form 16 January 2018; Accepted 26 January 2018
Available online 31 January 2018

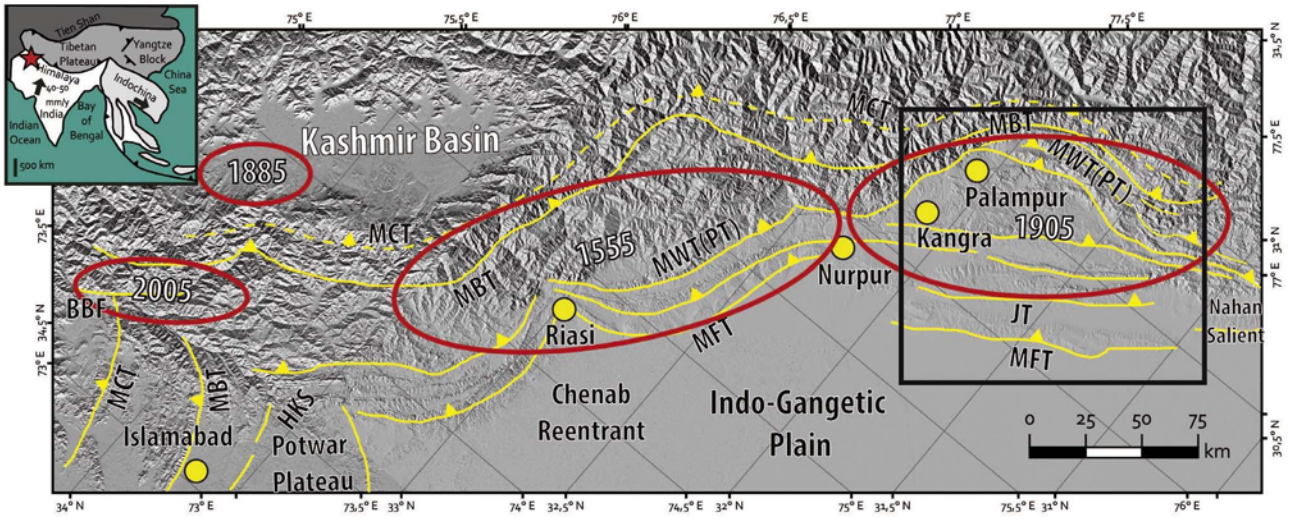

Fig. 1. General tectonic context for the Himalaya (Inset). The red star indicates the study area. The main map is a SRTM30 DEM (Rabus et al., 2003) view of the NW Himalaya depicting the first order thrusts identified by prior studies. Red ellipses approximately limit the main historical ruptures of earthquakes that have struck NW Himalaya. Ruptures for earthquakes before 1905 are depicted following previous authors (e.g. Ambraseys and Jackson, 2003; Avouac et al., 2006). The black square is the Kangra Reentrant. MFT = Main Frontal Thrust; JT = Jawalamukhi Thrust; MWT = Medlicott Wadia Thrust; PT = Palampur Thrust; MBT = Main Boundary Thrust; MCT = Main Central Thrust; HKS = Hazara-Kashmir Syntax; BBF = Balakot-Bagh Fault.

between CE 1165 and 1400.

In NW Sub-Himalaya, studies have demonstrated that some thrusts between the MBT and the MFT have accommodated, at the millennial time-scale, significant amounts of deformation. Gavillot et al. (2016), Vassallo et al. (2015), and Vignon et al. (2017) document, for the eastern flank of the Hazara-Kashmir Syntax (HKS in Fig. 1), that branches of the Medlicott-Wadia Thrust (MWT in Fig. 1) have accommodated shortening rates up to 11 mm/yr during the last tens of thousands of years at a distance of ~20 km from the MFT. These authors also demonstrate that motion on some of these thrusts has caused ~100 m fault scarps in Late Pleistocene–Holocene fluvial terraces, which is clear evidence of out-of-sequence deformation at the millennial timespan. In addition, ongoing out-of-sequence deformation has extensively been proposed in the NW Sub-Himalaya at the eastern flank of the HKS (Fig. 1), where the Balakot-Bagh Fault ruptured during the 2005 Mw 7.6 Kashmir Earthquake (Avouac et al., 2006; Kaneda et al., 2008; Kondo et al., 2008; BBF, Fig. 1). This event, and its severe consequences, raise the importance of assessing out-of-sequence deformation within the Sub-Himalayan Region.

The Kangra Reentrant (Figs. 1, 2a) is a convex-to-the-northeast U-shaped structure, where the NW Sub-Himalayan fold and thrust belt system reaches around 90 km width. The Kangra District, the political division to which this reentrant belongs, has not been struck by a major earthquake since the 1905 Mw 7.8 Kangra Earthquake (e.g. Ambraseys and Bilham, 2000; Fig. 1). Most of the studies related to the Kangra Earthquake state that its associated rupture did not reach the surface (e.g. Ambraseys and Bilham, 2000; Szeliga and Bilham, 2017); nevertheless Malik et al. (2015) suggest that the 1905 rupture reached the surface along the Kangra Valley Fault. For the Late Quaternary timespan, Dey et al. (2016) and Thakur et al. (2014) demonstrate that thrusts located at a distance up to 50 km from the active front have accommodated out-of-sequence deformation within the external Kangra Reentrant. As an example, the Jawalamukhi Thrust (JT; Figs. 1, 2a) deforms fluvial terraces of ca. 10 ka with a mean slip rate of 7.5 mm/yr (Dey et al., 2016).

The manifestation of Late Pleistocene-Holocene surface deformation has not been evaluated so far within the innermost part of the Kangra Reentrant, near the MBT (Fig. 2a). Here, hectometer-scale scarps deforming the Middle-Upper Siwaliks (Fig. 2b) are present, which may potentially be associated with seismogenic thrusts. This study focuses on a zone located between the Beas and the Neogad rivers, encompassing from the Jawalamukhi Thrust to the Main Boundary Thrust (Fig. 2a- and b), and undertakes a neotectonic survey aimed at recognizing and dating Late Quaternary deformation markers. Field observations and analysis of high-resolution Pleiades DEMs (0.5 m spatial resolution) were employed. From this analysis, fluvial terraces clearly disrupted by faults have been identified, which have produced metric-scale fault scarps. Samples for ^{10}Be concentration analysis were collected at the surface and along depth profiles within the terrace deposits; in this way, the ages of two terraces (TTa and TBa) were constrained. These results are discussed according to the state of knowledge concerning the seismotectonic regime of the Kangra Reentrant, a region that currently hosts a population of 1.5 million people. This work provides new field evidence of active deformation between the MFT and the MBT in the Kangra District, which could be later considered for a better evaluation of the seismic hazard in this Sub-Himalayan region of India.

2. Tectonic and geological context

The Himalayan orogeny started at 55 Ma as a consequence of the collision between the Eurasian and Indian plates (e.g. Le Fort, 1975). This convergence has been occurring at geological and geodetic rates of approximately 32 mm/yr in the northwestern Himalaya and 36 mm/yr in the eastern Himalaya (e.g. Ader et al., 2012; Bettinelli et al., 2006; DeMets et al., 1994, 1990). About 10–20 mm/yr of this bulk strain rate is accommodated in the Himalaya, while the rest is transferred to Tibet and southern Eurasia (e.g. Lyon-Caen and Molnar, 1985; Peltzer and Saucier, 1996). The fraction of the convergence transferred to the Himalaya has produced regional thrusting and large-scale crustal shortening, which has promoted the development of the fold-and-thrust belt that defines the foreland of this orogeny. Within this belt, tectonic deformation has been progressively migrating southwards since its inception (e.g. Gansser, 1964; Seeber et al., 1981; Fig. 1). Three main intracrustal thrusts developed: the Main Central Thrust (MCT) during Early Miocene (22–14 Ma; e.g. Metcalfe, 1993); the Main Boundary Thrust (MBT) during Late Miocene (9–11 Ma; e.g. Meigs et al., 1995); and the Main Frontal Thrust (MFT) during the Quaternary (< 2.5 Ma; e.g. Mugnier et al., 2004). These three main thrusts in the Lesser and Sub-Himalaya (Foreland Himalaya) are rooted at depth onto the Main Himalayan Thrust (MHT), which represents the basal regional detachment in this continent-continent collision scenario (e.g. Duputel et al.,

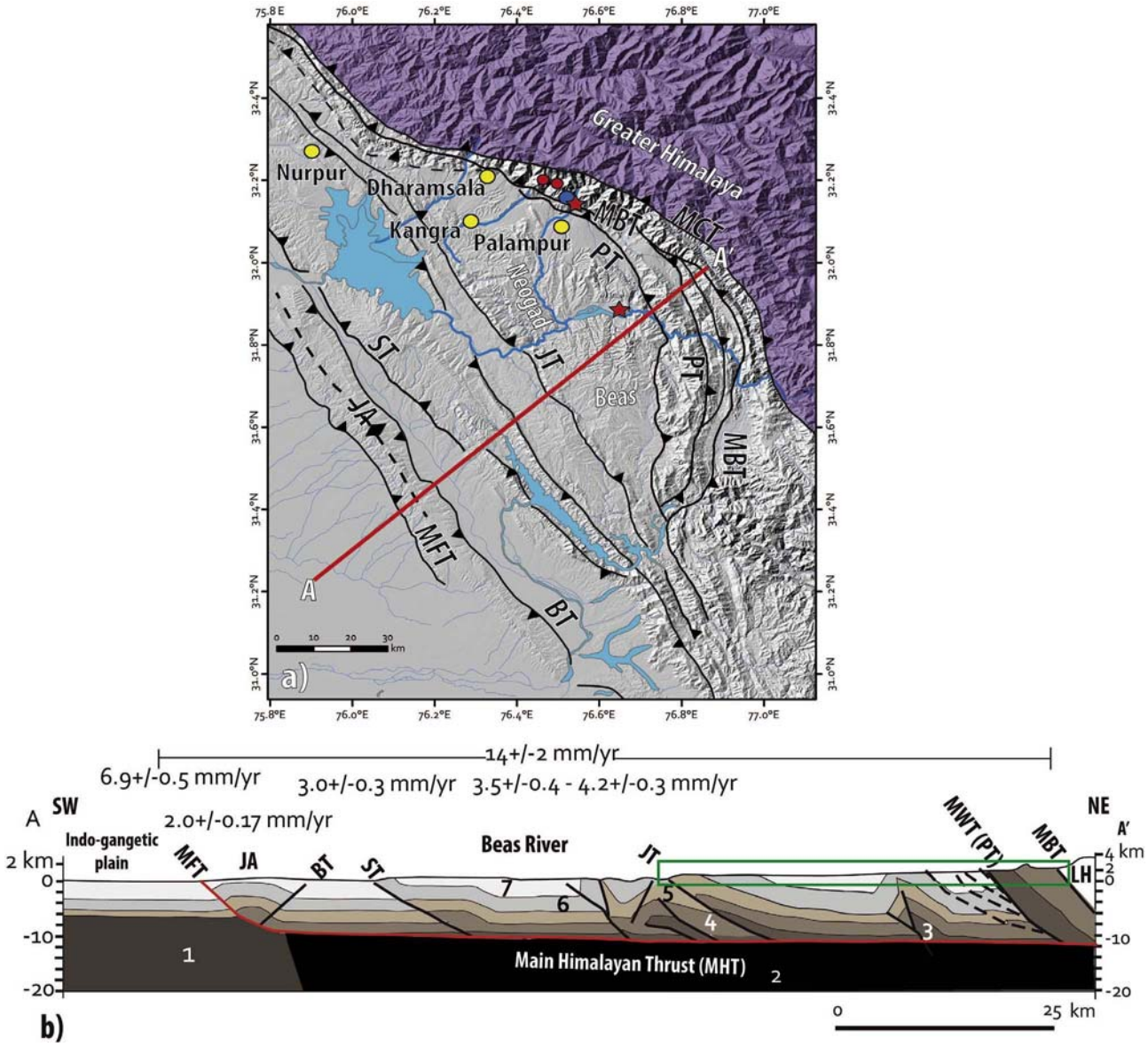

Fig. 2. (a) Detailed view of the Kangra Reentrant and the main thrusts accommodating deformation between the Beas and Neogad rivers. MFT = Main Frontal Thrust; MBT = Main Boundary Thrust; MCT = Main Central Thrust; JA = Janauri Anticline; ST = Soan Thrust; JT = Jawalamukhi Thrust; PT = Palampur Thrust. Red and blue circles are the sites where the MBT and the PT are analyzed. Red stars are the sites where the fault scarps were observed. (b) Schematic cross-section AA′ indicated in (a). Based on Powers et al. (1998) and Thakur et al. (2014). It shows the main thrusts accommodating deformation in the Kangra Region. Shortening velocities are from Thakur et al. (2014). The rectangle in the segment of the cross-section corresponds to the study area. MFT = Main Frontal Thrust; JA = Janauri Anticline; ST = Soan Thrust; JT = Jawalamukhi Thrust; PT = Palampur Thrust; MBT = Main Boundary Thrust. 1. Pre-Cambrian Crystalline Basement; 2. Pre-Cambrian–Cambrian metasedimentary rocks; 3. Lower Dharamsala; 4. Upper Dharamsala; 5. Lower Siwalik; 6. Middle Siwalik; 7. Upper Siwalik. In this cross-section, colors are only for better identifying the former units.

2016; Zhao et al., 1993; Fig. 2b). Each of the main intracrustal faults within the Foreland Himalaya marks the limit of individualized geological units (e.g. Gansser, 1964; Fig. 2a and b) that are, from north to south: (a) *The Greater Himalaya* (GH; e.g. Gansser, 1983; Fig. 2a); (b) *The Lesser Himalaya* (LH; e.g. DeCelles et al., 1998; Yin, 2006; Fig. 2(b) and (c) *The Sub-Himalaya*. Rocks of this latter unit outcrop in the study area. Murree (Oligo-Miocene) and Siwalik (Plio-Pleistocene) formations pertain to the Sub-Himalaya (Fig. 2b). Murree rocks, originally named Dharmsala Formation (e.g. Karunakaran and Rao, 1979), have been classified as clays and siltstones (Lower) and sandstones (Upper). To their southern end, Murree rocks overthrust the Siwalik Formation by the occurrence of the MWT, locally named Palampur Thrust (PT; Thakur et al., 2010). The Siwalik Formation has been divided into three parts: (i) The Lower Siwalik, mainly composed of alternating sandstones and claystones, with minor siltstones and pebble horizons; (ii) the Middle Siwalik, corresponding to sandstones with minor claystones, and prominent conglomerates close to the MBT; and (iii) the Upper Siwalik, including conglomerates with increasing sandstones away from the MBT (e.g. Karunakaran and Rao, 1979). The southern bound of the Sub-Himalaya is the MFT, which conducts overthrusting of the Tertiary units above the alluvial Indo-Gangetic plains.

3. Earthquakes in NW Himalaya

The NW Himalaya of India and Pakistan has been struck by strong to great earthquakes ($7 \leq Mw < 8$) during historical times (Fig. 1). Some of these great historical earthquakes are, in general, well characterized through the analysis of historical testimonies. However, events such as the ca. 1400 Chandigarh Earthquake (see below) have been only characterized from paleoseismological studies, implying that the seismic catalogue for this region is probably incomplete, even concerning such strong events. Some of the best recognized historical

earthquakes in NW Himalaya are:

(a) *The ~ 1400 Chandigarh Earthquake*. This great earthquake, only known through paleoseismological investigations, involved from 3.5 m up to 16 m of slip at the surface along the MFT (e.g. Jayangondaperumal et al., 2013; Kumar et al., 2005; Malik et al., 2008).
(b) *The 1555 M ~ 7.6 Srinagar Earthquake*. Although scarce details are available in literature, it has been suggested that this earthquake caused severe destruction along the Kashmir Valley (e.g. Ambraseys and Jackson, 2003).
(c) *The 1803 Mw 7.5–8 Kumaon Earthquake*. The 1803 Kumaon Earthquake has been studied by Ambraseys and Jackson (2003), who estimated a Mw of 7.5 for this event. Their Mw suggestion is based on the damage record made by British officers visiting the region shortly after the earthquake. Ambraseys and Douglas (2004), by re-assessing intensities and isoseismals, propose that the 1803 earthquake reached Mw of 8. Its epicentral location has been suggested to be ~200 km eastward from the study area. According to Rajendran and Rajendran (2005), this earthquake did not reach the surface along the MFT.
(d) *The 1885 Mw 6.3 Kashmir Earthquake*. The 1885 Kashmir Earthquake produced, according to Ahmad et al. (2013), a ~50 km long surface rupture. Ambraseys and Douglas (2004) assigned a Mw of 6.3 for this event. The suggested rupture extent associated with this earthquake is represented in Fig. 1, following Joshi and Thakur (2016).
(e) *The 1905 M ~ 7.8 Kangra Earthquake*. Based on re-measurements of historic triangulation points within the proposed epicentral region, it has been suggested that this earthquake involved a rupture that extended approximately from the Jawalamukhi Thrust (JT) to the present day locked line along the MHT, beneath the Greater Himalaya (Wallace et al., 2005; Szeliga and Bilham, 2017; Fig. 1). Furthermore, it has been proposed that this earthquake did not produce any surface rupture (e.g. Ambraseys and Bilham, 2000). Nevertheless, Malik et al. (2015), on the basis of a paleoseismic study, infer that surface rupture of the 1905 earthquake is represented by a right lateral strike-slip fault, named Kangra Valley Fault.
(f) *The 1974 Patan Earthquake*. This very destructive earthquake (causing 1000 fatalities and destroying 18,000 houses) was first studied by Ambraseys et al. (1975), who estimated a Mb of 6.0. In Jackson and Yielding (1983), it is suggested that the Patan Earthquake occurred at 10 km depth with a reverse mechanism, at the eastern part of the 2005 Kashmir Earthquake rupture area. No surface rupture was observed following this event.
(g) *The 2005 Mw 7.6 Kashmir Earthquake*. This event was produced by a fault within the Sub-Himalaya, the Balakot-Bagh Fault (Fig. 1), and caused a surface vertical separation with a maximum of ~7 m (e.g. Avouac et al., 2006; Kaneda et al., 2008).

Strong-to-major earthquakes (Mw < 8) have been interpreted to be restricted by active faults (ramps) within the Sub-Himalaya, such as the MWT and the JT. These thrusts branch off at depth from the MHT. Ruptures linked to these kind of earthquakes would have the potential to reach the surface (Mugnier et al., 2013). A recent example of this style of earthquake is given by the 2005 Mw 7.6 Kashmir Earthquake (Avouac et al., 2006; Kaneda et al., 2008; Kondo et al., 2008). This event constitutes evidence of the seismic potential linked to out-of-sequence deformation in NW Himalaya. In addition, Mw < 8 earthquakes have also occurred solely on the MHT, as represented by the 25 April and 12 May 2015 Nepal earthquakes (Parameswaran et al., 2015). In turn, great earthquakes (Mw > 8), as was likely the ~1400 event (e.g. Jayangondaperumal et al., 2013), would nucleate along the MHT, affect its whole brittle domain, and emerge along the MFT (Mugnier et al., 2013).

4. Structural setting for the Kangra Reentrant

Thrusts within this structure (Figs. 1, 2a) have been studied in detail by prior investigators (e.g. Malik et al., 2015; Powers et al., 1998). In the Sub-Himalayan domain, it encompasses a maximum width of ~90 km, where thrusts and folds accommodate deformation between the MBT and the MFT (Fig. 2b). According to Powers et al. (1998), in this reentrant, the MBT suffers a change in its orientation from southeast to east trending, as the MFT jumps southwestward. In the southern-outer part of the reentrant, faults and fold axes are mostly parallel to the MFT, while to its northern-inner extent these follow the trend of the MBT (Fig. 2a).

Shortening rates for the Kangra Reentrant have been constrained to 14 ± 2 mm/yr from balanced cross-sections for the long-term (Powers et al., 1998). For the MHT, based on GPS measurements (Banerjee and Burgmann, 2002; Kundu et al., 2014), a slip rate of 14 ± 1 mm/yr along the ductile part has been determined. This similarity allows Late Quaternary slip rates to be considered as a proxy for long-term rates along the MHT (Thakur et al., 2014). This is supported by the documented steady convergence between India and Eurasia over the geological time scale (Bettinelli et al., 2006; DeMets et al., 2017; Patriat and Achache, 1984).

Fig. 2b is a simplified schematic cross-section based on Powers et al. (1998) and Thakur et al. (2014) for two NE trending transects west and east of Kangra City. From south to north, the most active structures documented in the literature for the Kangra Reentrant, between the MFT and the MBT, are the Janauri Anticline (JA), the Soan Thrust (ST), the Jawalamukhi Thrust (JT) and the Palampur Thrust (PT). Thakur et al. (2014) have estimated that the MFT has accommodated a slip rate of 6 mm/yr during the last 42 ka; furthermore, the ST and JT have accommodated slip rates of 3 mm/yr over the last 29 ka and 3.5–4.4 mm/yr during the last 32–30 ka, respectively. Malik and Mohanty (2007) suggest that these faults are important for developing the present complex landscape of the Kangra Reentrant and, in general, of the NW Sub-Himalaya. In the study area, an example of this phenomenon is given by the PT, which at least partially defines the main mountain front of the reentrant. Outer thrusts, like the ST and JT, have also produced hectometer scarps that define the front of mountain ranges in the Sub-Himalaya of the Kangra Reentrant below 1500 m a.s.l. (Fig. 2b).

5. Fluvial terraces as markers of neotectonic deformation

The Beas and Neogad rivers limit the study area to the east and , respectively (Fig. 2a). These rivers, and their tributaries, have produced several fluvial terraces presently preserved between ~1600 and ~650 m a.s.l. In general, terrace deposits consist of conglomerates over the Sub-Himalaya molasses (Siwaliks). Two of these terraces, in addition to the thalwegs of the rivers that promoted their formation, preserve evidence of neotectonic deformation (Figs. 3–7).

At a site located at ~3 km north of Palampur (site i in Fig. 3a- and b), a fluvial terrace at ~1620 m a.s.l., formed by a tributary of the Neogad River, was identified and named TTa terrace (Fig. 3a–e). Its surface is disrupted by a fault scarp of ~3.6 m height; this scarp is labelled as Goat Scarp (Fig. 3b, d and e). The Goat Scarp is oriented N35°W and was formed in debris flow deposits, at least 10 m thick, both at the upthrown and downthrown block; in-depth, this deposit includes Sub-Himalaya pebbles and boulders of up to 1 m in diameter. At the surface, both on the upthrown and downthrown blocks, boulders of up to 2 m in diameter can be recognized (Fig. 3d). The causative thrust was also identified as affecting basement rocks (Sub-Himalaya), as depicted in Fig. 3c. The Goat Scarp represents the evidence of recent fault activity the furthest from the MFT in the study area, at around 80 km northwards. The displaced terrace has slopes of 18°S and 15°S in the hanging and the footwall block, respectively. Such a high inclination may be due to the high density of the causative debris flow. The upper

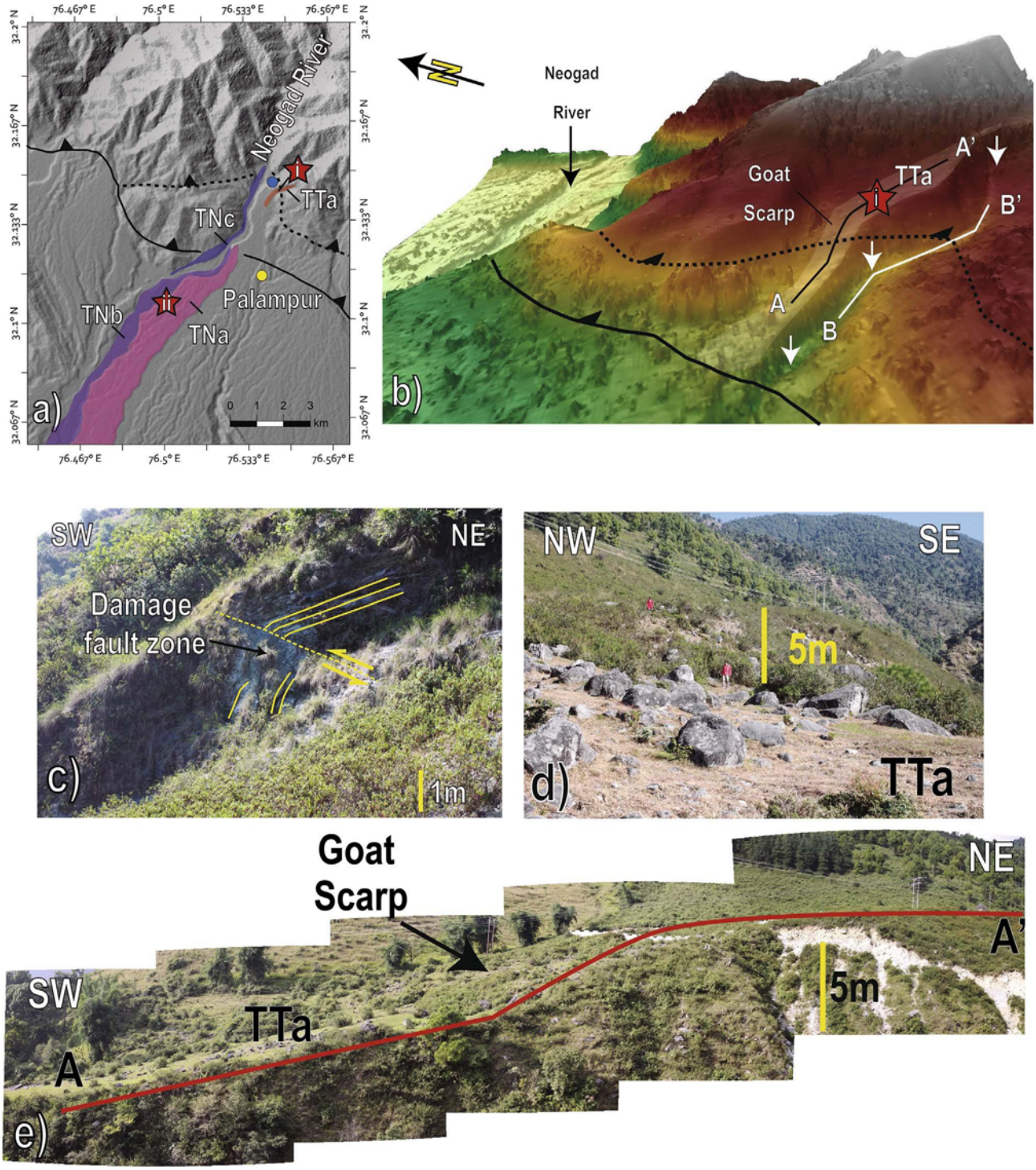

Fig. 3. (a) Map depicting the TTa, TNa, TNb and TNc (see main text) in the periphery of Palampur; i and ii in red stars are observation/sampling sites. PT is the Palampur Thrust. The blue circle indicates the site of (c). AA' and BB' are the profiles shown in Fig. 4. (b) 3D view of the morphological context for TTa. The white shaded area approximately marks the TTa extent. Topographic profiles of Fig. 4 are also depicted. (c) The thrust producing the Goat Scarp further NW, as depicted by the blue circle in (a), affecting Sub-Himalaya rocks. Solid yellow lines indicate bedding. (d and e) View of the Goat Scarp in the TTa Terrace.

half of the scarp profile is dominated by a slope of 27°S, while its lower half exhibits a slope of 19°S (Fig. 4a). From field observations, given the impossibility of trenching in this boulder-rich deposit environment, it was not possible to determine if this scarp corresponds to a single or multiple seismic ruptures along the causative fault. This thrust also produced a knick point in the tributary river that limits the TTa terrace to the SE (Fig. 4b).

Southwestward of site i, three other terraces between ~1120 and 1100 m a.s.l. were identified, named TNa, TNb and TNc respectively (site ii in Fig. 3a); the three terraces were formed by the Neogad River. Terraces TNa and TNb preserve evidence of an extremely degraded fault scarp; this scarp may have been evolved by a currently inactive thrust, represented by the segmented line in the periphery of site ii (Fig. 3a). Terrace TNc is the youngest terrace identified along the Neogad River and is not disrupted by fault scarps. Further south, between the PT and the JT, no significant localized deformation affecting

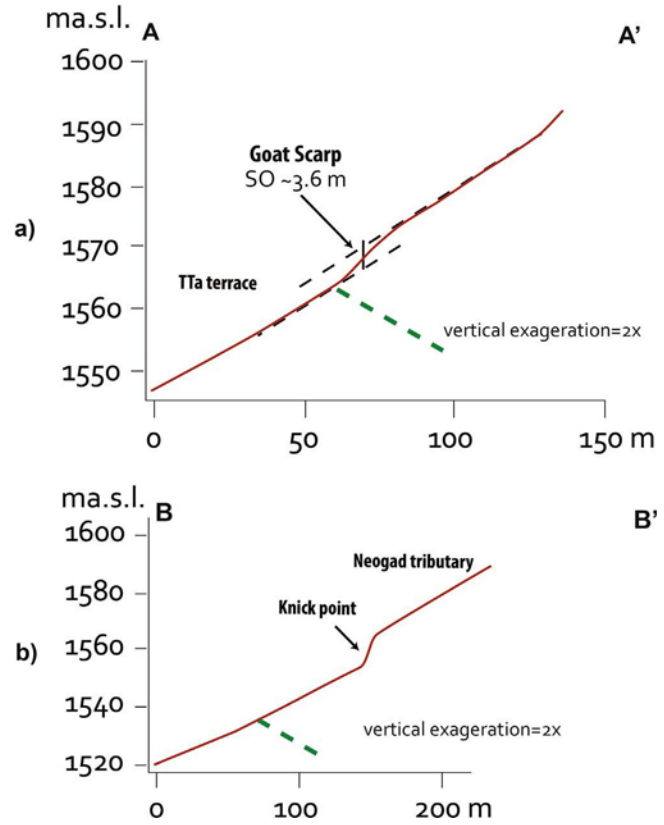

Fig. 4. AA′ and BB′ are topographic profiles of Pleaides DEM (0.5 m resolution) depicted in Fig. 3a and b. (a) Topographic profile across the Goat Scarp. (b) Topographic profile along the tributary river limiting the TTa terrace to the SE. SO is the surface offset.

terraces was observed.

Further east, at site iii of Fig. 5a, a fluvial terrace at ~652 m a.s.l. was identified, formed by the Beas River, named TBa. This predominantly-flat terrace is markedly deformed by the Dharampur Scarp (Fig. 5b–e), with ~3.5 m height and oriented N10°E. In comparison with the Goat Scarp, the Dharampur Scarp has a less sharp morphology and may attest to older seismic rupture event(s). At both sides of the scarp the TBa terrace is preserved over a fluvial conglomerate deposit of at least 25 m thickness. At the surface, both on the upthrown and downthrown blocks, clasts no more than 0.5 m in diameter were observed (Fig. 7c). In-depth, clasts composing this deposit are pebbles and boulders of Sub-Himalaya rocks (Fig. 7d). The thrust causing this scarp was clearly observed in the TBa flank as shown in Fig. 5f. The site at which the fault scarp was identified is located at around 75 km north of the MFT. The terrace surface disrupted by this scarp is almost horizontal at both the hanging and footwall (Figs. 5c and d, 6a and b). The scarp appearance is disturbed by anthropic activity but in topographic profiles a very irregular slope of ~22°W is observed (Fig. 6a and b). Along the Beas River, following the trend of the Dharampur Scarp, two knick points were identified; these were interpreted as formed by the causative thrust (Fig. 6c).

6. ^{10}Be concentrations from fluvial terraces and age estimation

In situ produced CRN (herein ^{10}Be) can be used to measure the duration of surface exposure to cosmic rays (c.f. Gosse and Phillips, 2001) and thus provide a numerical age of a surface. These ages must be considered approximate because of their dependency on parameters like prior exposure issues (inheritance; e.g. Anderson et al., 1996) and post-depositional effects such as erosion (e.g. Gosse and Phillips, 2001). Other parameters affecting surface cosmogenic isotope production are the latitude and elevation of the sample sites; both are positively correlated with isotope production (Lal, 1991). Since these terraces are claimed to be formed during Late Pleistocene–Holocene, based on former studies in NW Himalaya (e.g. Bookhagen et al., 2006; Dey et al., 2016; Vassallo et al., 2015; Vignon et al., 2017), long-term oscillations of ^{10}Be production are considered to be negligible for these calculations. At a given depth (x) and for a material density (ρ), the production rate (Px) can be estimated if the surface production rate (P0) is known (Lal, 1991):Wwhere Λ is the characteristic attenuation factor, which is roughly invariant at different locations on Earth (Lal, 1991).

Samples from the TTa and TBa terraces were collected in order to constrain the age of the deformation in this part of the Kangra Reentrant. To determine exposure ages, depending on the availability and coherence (size and lithology) of the target materials, individual and amalgamated samples were collected. Individual samples correspond to boulders and pebbles of quartz, granite, and gneiss that were collected both atop of the terrace deposits and along vertical profiles (Figs. 7 and 8). For surface samples, when available, chip samples were extracted from semi-buried blocks greater than 1.5 m in diameter. In contrast, amalgamated samples correspond to ~30 single rounded pebbles of quartz and/or the aforementioned lithologies, with sizes of less than 5 cm in diameter. Following the methodology of Anderson et al. (1996), samples along a vertical profile (one per level) were collected to around 3.5 m depth in terraces TTa and TBa, in order to estimate the amount of inherited ^{10}Be due to prior exposure processes of the clasts. The vertical profile for TTa was carried out along a recently opened road cut wall. For TBa, the vertical profile was made in a site of the terrace riser recently affected by landslides. Thus, for both cases, the influence of lateral cosmic rays in ^{10}Be production is neglected. Clasts coming from the Himalayan front were collected; in the study area, units of the Sub-Himalaya are exposed at this front. Samples are assumed to have not been remobilized after their deposition, since they are partially buried and terrace sediments show the typical fabric related to the causative original processes (debris flow for TTa and fluvial regime for TBa). Cosmogenic ages for similar fluvial terraces in NW Himalaya have resulted in Late Pleistocene-Holocene ages (e.g. Dey et al., 2016); for such a period, only strong surface denudation would significantly affect the exposure ages. For example, an erosion rate of 1 m/ka may artificially increase by ~10% a 100 ka age (e.g. Owen et al., 2006). Regardless, the aspect of the targeted terraces is dominantly flat and often exhibits a fine-grained cover, which suggests that this factor may be neglected for age calculations.

Mechanical and chemical sample preparation was carried out in the Cosmogenic Laboratory of the ISTerre (Chambéry and Grenoble, France). The protocol for chemical treatment of samples follows the same as Vassallo et al. (2015). Measurements for ^{10}Be were performed at the accelerator mass spectrometry facility ASTERISque (Aix-en-Provence, France (Arnold et al., 2010)). ^{10}Be concentration uncertainties include analytical uncertainties from the counting statistics, instrumental variability (1%) and chemical blanks. Production rates were calculated with the Cronus calculator v2.3 (Balco et al., 2008) using the scaling model of Lal (1991) and Stone (2000), and geomorphic shielding factors of (Dunne et al., 1999).

Seven samples were obtained from one site in the TTa Terrace, and four samples from one site in the TBa Terrace. Sample details and ^{10}Be results are given in Table 1. For both cases, Hidy's method (Hidy et al., 2010) was performed. The employed version is the one modified by Ruszkiczay-Rüdiger et al. (2016) to take into account the theoretical muogenic production of Braucher et al. (2011). This method uses a Monte Carlo simulation to model TCN depth profiles, considering the propagation of all error sources, for calculating the most probable values for age, inheritance and erosion rate. With this, several profile curves that can explain TCN concentrations in the subsurface are obtained (Fig. 8a and b); valid solutions are those with $\chi^2 \leq \chi^2_{min} + 1$ (e.g. Braucher et al., 2009; Delmas et al., 2015) which is considered as equivalent to 1-sigma confidence interval (Bevington and Robinson,

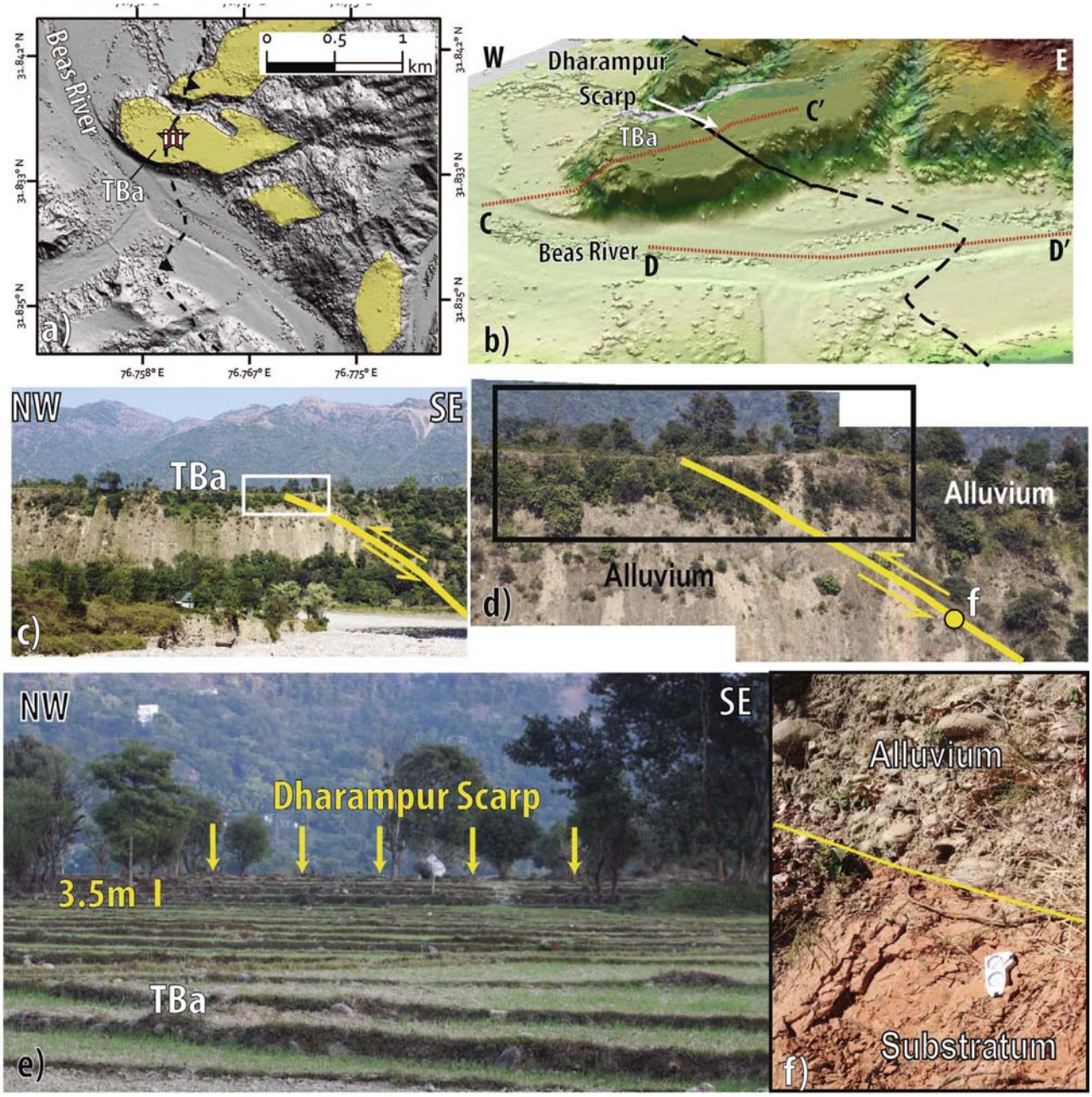

Fig. 5. (a) Map view of the TBa; iii indicates the sample site (^{10}Be) on this terrace. CC′ and DD′ are topographic profiles shown in Fig. 6; (b) Inclined 3D view of the terrace and interpreted trace of the fault producing the Dharampur Scarp; (c and d) Panoramic views of the TBa terrace and Dharampur Scarp. White and black rectangles indicate the same area in both photos; (e) Frontal view of the Dharampur Scarp; (f) Causative thrust cutting Quaternary alluvium deposits. The substratum is affected by the thrust forming an intense damage zone (red level). (For interpretation of the references to colour in this figure legend, the reader is referred to the web version of this article.)

2003). Therefore the chi square, $\chi^2 = \sum_{i=0}^{n} \left(\frac{C_i - C_{(xi,t)}}{\sigma_i}\right)^2$, was calculated (where n: number of samples; Ci: measured ^{10}Be concentration at depth xi for sample i; and C (xi, t): modelled ^{10}Be concentration at depth xi; and σi: analytical uncertainty at depth xi). In Fig. 8a and b, the left side diagrams depict the possible solutions, while those to the right indicate the best solution considering zero erosion. From the best solutions, the mean age associated with a mean inheritance for each case was calculated; a mean age of 6.2 ka with a mean inheritance of ~10% for the TTa Terrace, and a mean age of 7.5 ka with a mean inheritance of ~15% for the TBa terrace, were obtained.

7. Discussion

The analyzed metric-scale fault scarps demonstrate that out-of-sequence deformation has occurred during the last ca. 7.5 ka in the innermost Kangra Reentrant. This kind of deformation is evident very close to the MBT in the study area, ~80 km northward of the MFT. This is the first time that Holocene out-of-sequence deformation is reported at such an inner position in the Kangra Reentrant.

The fact that terraces TTa and TBa are dislocated by different branches of the PT may signify that, in the studied area, millennial-scale deformation does not tend to concentrate along one single thrust but, on the contrary, is distributed among several strands in a zone of ~15 km width. Consequently, the formation of hectometer fault scarps defining high mountain ranges is unlikely. Instead, slip occurs along several fault strands as, for example, in the Chenab Reentrant (Mugnier et al., 2017), or in the more external zones of the Kangra Reentrant as along the JT (Thakur et al., 2014).

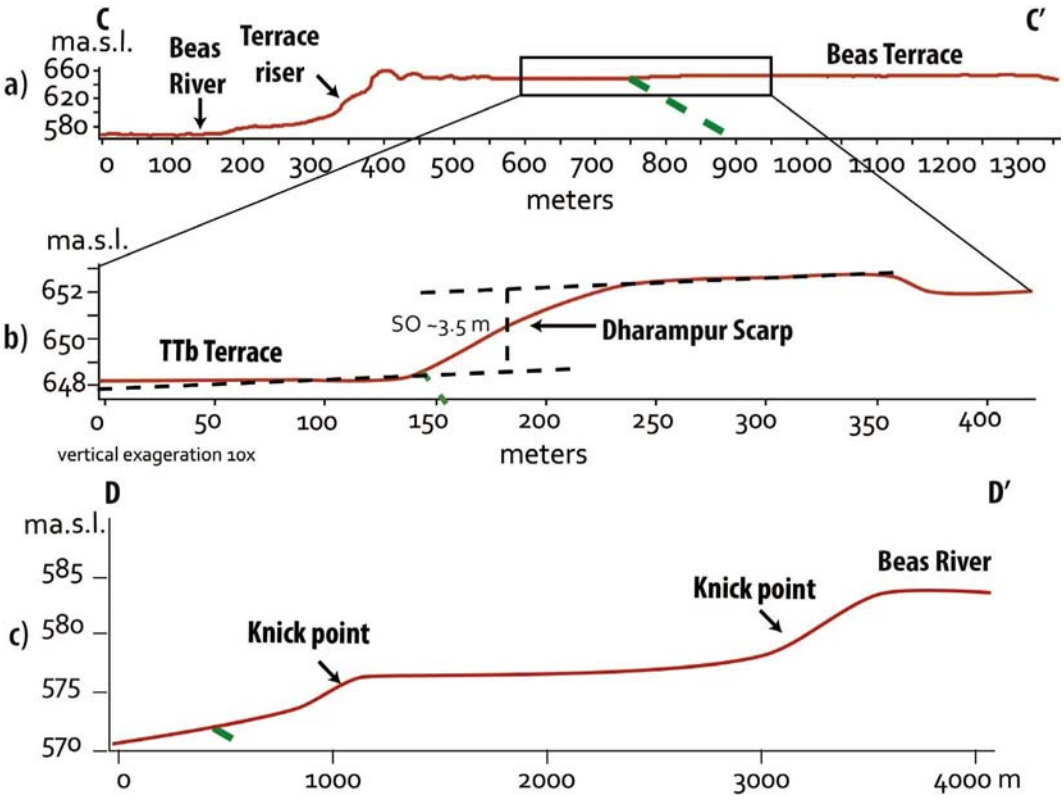

Fig. 6. (a and b) Topographic profiles across the Dharampur Scarp and (c) Topographic profile along the Beas River in the periphery of the deformed TBa terrace. Green segmented lines indicate the interpreted location of the causative thrust. SO is the surface offset. The sites where the profiles were conducted are indicated in Fig. 5b.

With the available evidence, it is neither possible to clarify if the identified scarps were formed by one or more discrete slip events, nor possible to estimate the age of the last causative event. Nevertheless, it is proposed, based on their degraded morphology, that they do not correspond to the surficial expression of the Kangra Earthquake. This interpretation agrees with the suggestions of Hough et al. (2005) who, based on a reevaluation of the macroseismic field proposed for this event, along with the study of geodetic observations and the original seismograms, interpret a blind rupture restricted to the MHT for the 1905 earthquake. Also, this is congruent with the early field observations related to this event in 1905, as reported by Bilham and Wallace (2006).

From scarp-offset measurements, the total slip accommodated by the two different thrusts deforming terraces TTa and TBa is ~7 m for the last ca. 7.5 ka. If this total slip is considered as a proxy of the slip induced by the causative earthquakes, a cumulative deformation rate of ca. 1 mm/yr may be estimated for this interval; this is ~10% of the total strain distributed within the entire Kangra Reentrant (Banerjee and Burgmann, 2002; Powers et al., 1998). Although roughly determined, this strain rate estimation, in addition to those made by Dey et al. (2016) and Thakur et al. (2014), allows the interpretation that Holocene deformation is significantly distributed over a wide area along thrusts that emerge at the surface. The Kangra and Kashmir reentrants are one of the few places along the Himalayan orogeny where strain is distributed within such a wide region. The question of why this happens in the Kangra Reentrant remains open. Mugnier et al. (1999) suggested that the distribution of deformation within and around intramountain basins, like the studied area, is linked to the interaction between erosion, sedimentation, and tectonics in a wedge characterized by a steep basal slope. Another possibility is the occurrence of crustal-scale lithological contrasts within the Sub-Himalaya of the Kangra Reentrant, which has also been proposed as a factor enhancing out-of-sequence deformation (Mukherjee, 2015). Similar vestiges of distributed deformation in other similar places along the Sub-Himalaya may have been eroded or not yet found.

Based on the data presented in this study and prior literature (Mugnier et al., 2013; Seeber and Armbruster, 1981), it is proposed that active deformation in the Kangra Reentrant may be undertaken by three kinds of ruptures:

(a) The first type of rupture is given by 1905 Kangra-like events, which would correspond to deep strong-to-major size earthquakes ($7 \geq Mw < 8$), restricted to the portion of the MHT located beneath the Sub-Himalaya (Fig. 9a; *sensu* Wallace et al., 2005). This kind of rupture would not have the capacity of reaching the surface but, instead, may strengthen the occurrence of earthquakes along the shallowest portions of the MHT and, eventually, emerge at the surface along the MFT. An analog to these ruptures is given by the 25 April and 12 May 2015 Nepal earthquakes (Parameswaran et al., 2015).

(b) The second type of rupture is represented by the Chandigarh ~1400-like events, which involve more than 15 m of coseismic slip (Jayangondaperumal et al., 2013). This kind of earthquake would be produced at the deeper half of the MHT and have the necessary energy to get to the surface along the MFT (Fig. 9b). They probably represent the worst-case scenario, in terms of the expected Mw ($Mw \geq 8$), for the seismic hazard appraisal for the Kangra Reentrant. These kind of earthquakes may also be similar to the 1934 Bihar-Nepal rupture, which reached the surface along the MFT (Sapkota et al., 2013).

(c) The third type of rupture is nucleated at the brittle/ductile transition of the MHT and propagated along ramps within the fold-and-thrust belt of the Kangra Reentrant. They would be the causative earthquakes for the scarps that are documented in this study (Fig. 9c). This kind of rupture may be similar in magnitude to those of the first type but would have the potential of reaching the surface and producing fault scarps such as those reported in this work. It is hypothesized that the causative earthquakes for these scarps may be

Fig. 7. (a) View of the site where depth samples for TTa were collected. (b) Boulders from which chip surface samples were extracted for TTa. (c) View of the TBa surface aspect. (d) Downhill view of the TBa terrace flank, from which in-depth samples were collected. The red arrow indicates the downward slope of the flank.

similar to the 2005 Mw 7.6 Kashmir Earthquake (Avouac et al., 2006; Kaneda et al., 2008; Kondo et al., 2008).

Considering the evidence of out-of-sequence deformation within the outer Kangra Reentrant (Dey et al., 2016; Thakur et al., 2014) and the herein presented results, it is proposed that the width of the seismogenic part of the Main Himalayan Thrust (MHT) covers at least 80 km width beneath this reentrant. This is roughly consistent with the position of the locking line determined by Jouanne et al. (2017) for modelling slip along the MHT by using GPS data. Furthermore, it is suggested that all the active thrusts identified between the MFT and MBT in this reentrant have the potential to cause ruptures of the third style (Fig. 9c). In the particular case of the inner reentrant nearby Palampur, it is interpreted that the cumulative slip rate of ca. 1 mm/yr, estimated for the last 7.5 ka, is the result of earthquakes propagating along thrusts (ramps) connected at depth to the MHT. Unfortunately, the characterization of the seismic cycle along single thrusts has not yet been possible and this limits the assessment of their associated seismic potential. Additional information about aspects such as recurrence times of earthquakes along individual out-of-sequence thrusts would permit the evaluation of more complex scenarios involving, for instance, simultaneous reactivation of two or more faults. With the available evidence, this possibility should not be ruled out. Even if the earthquakes, causing out-of-sequence deformation, may not have great/large magnitudes (Mw < 8), they may result in a severe impact for densely inhabited areas located in the periphery, as proved by the 2005 Mw 7.6 Kashmir Earthquake.

Conclusions

- Two fluvial terraces -TTa and TBa- in the innermost Kangra Reentrant, at ~80 km north from the Main Frontal Thrust, are deformed by different branches of the Medlicott-Wadia Thrust, locally named Palampur Thrust. Deformation is represented by metric-scale fault scarps.
- Terraces TTa and TBa represent examples of climatically-formed terraces that have been successively deformed by tectonic effects.
- ^{10}Be age determinations for these terraces show that deformation

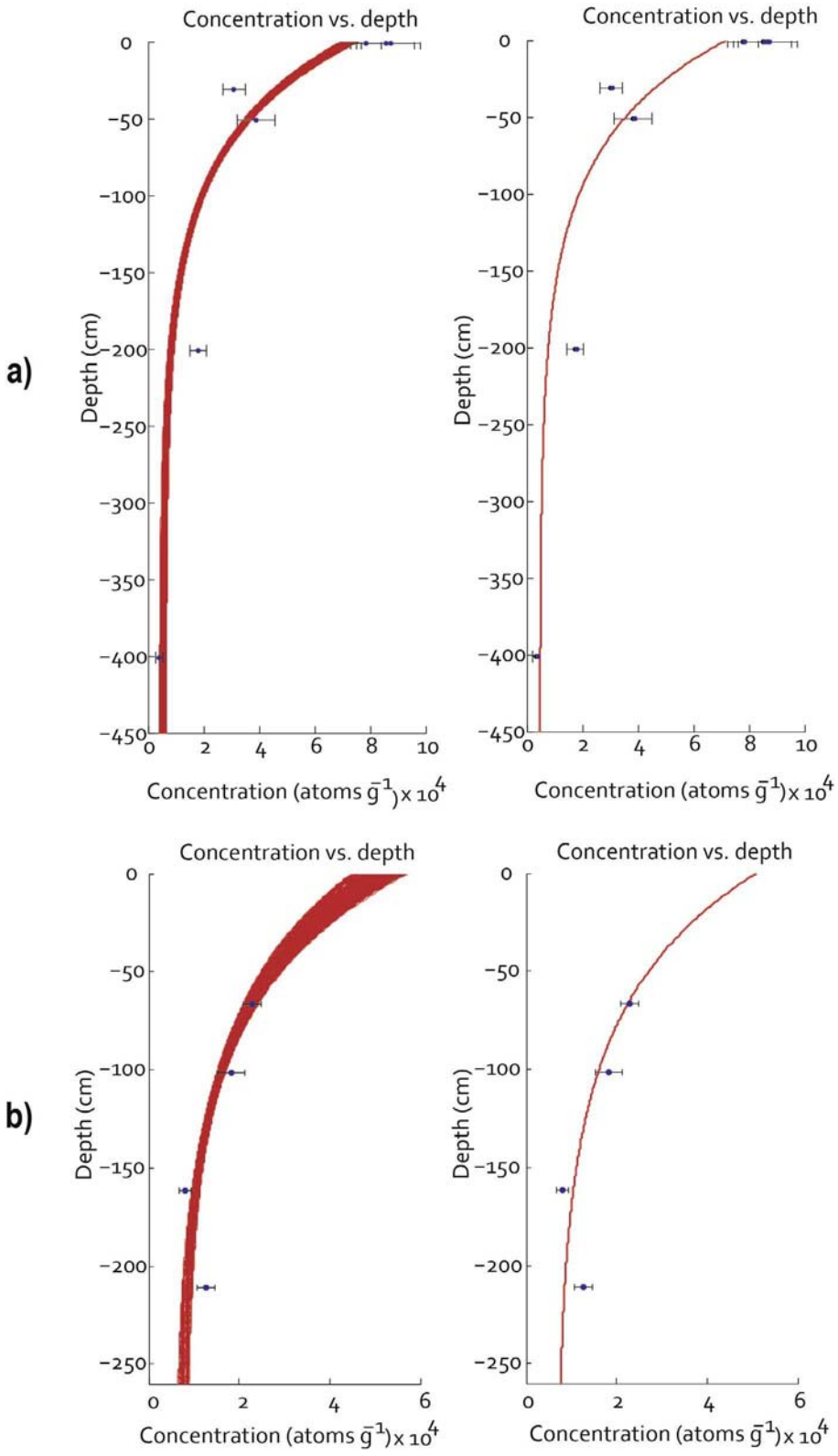

Fig. 8. (a and b) left. Possible solutions for TCN profile in TTa and TBa, respectively. Inheritances of ~10% and ~15% were determined for TTa and TBa determinations, respectively. (a and b) right. The best solution for each model.

within the innermost reentrant has occurred after ca. 7.5 ka; this is clear evidence of out-of-sequence deformation over the millennial time-scale.

- Surface offset produced along different branches of the Palampur Thrust during the last ca. 7.5 ka results in a cumulative shortening rate of ca. 1 mm/yr for this timespan. This estimation is around 10% of the bulk-strain accommodated by the whole Kangra Reentrant during the Late Quaternary and even during the Holocene.
- It is considered that the estimated cumulative slip rate may be dissipated during earthquakes (Mw < 8) triggered at the brittle/

Table 1
^{10}Be concentration data. Pressure has been estimated using the offline Matlab code from Cronus calculator (NECPatm_2.m). From the Monte Carlo simulations for TTa and TBa profiles, Xchi min parameters of 33.6 and 9.6, respectively, have been determined.

Sample	Terrace	Composition/Size	Latitude	Longitude	Elevation [m a,s,l,]	Depth [m]	Sample thickness (cm)	[10Be] at/g	Uncertainty [10Be] at/g	Uncertainty [10Be] %	Shielding Factor	Surface P0(at/g/yr)
BE-14-21	TBa	Granite boulder	31.835	76.760	683	0.65	2.5	22,825	1910	8.368	1.000	6.7
BE-14-17	TBa	Granite boulder	31.835	76.760	683	1	2.5	18,271	3013	16.491	1.000	6.7
BE-14-19	TBa	Granite boulder	31.835	76.760	682	1.6	2.5	8087	1283	15.865	1.000	6.7
BE-14-18	TBa	Granite boulder	31.835	76.760	682	2.1	2.5	12,632	1911	15.128	1.000	6.7
BE-14-39	TTa	Granite boulder	32.143	76.547	1614	0	2.5	87,489	10,475	11.973	0.943	13.2
BE-14-40	TTa	Granite boulder	32.143	76.547	1614	0	2.5	78,599	5499	6.996	0.943	13.2
BE-14-41	TTa	Granite boulder	32.143	76.547	1614	0	2.5	85,659	10,425	12.170	0.943	13.2
BE-14-42	TTa	Quartz pebbles (30)	32.143	76.547	1613	0.3	2.5	30,980	4066	13.125	0.943	13.2
BE-14-43	TTa	Quartz pebbles (30)	32.143	76.547	1612	0.5	2.5	38,888	6909	17.766	0.943	13.2
BE-14-44	TTa	Quartz pebbles (30)	32.143	76.547	1612	2	2.5	18,011	2997	16.640	0.943	13.2
BE-14-45	TTa	Quartz pebbles (30)	32.143	76.547	1610	4	2.5	4056	1435	35.380	0.943	13.2

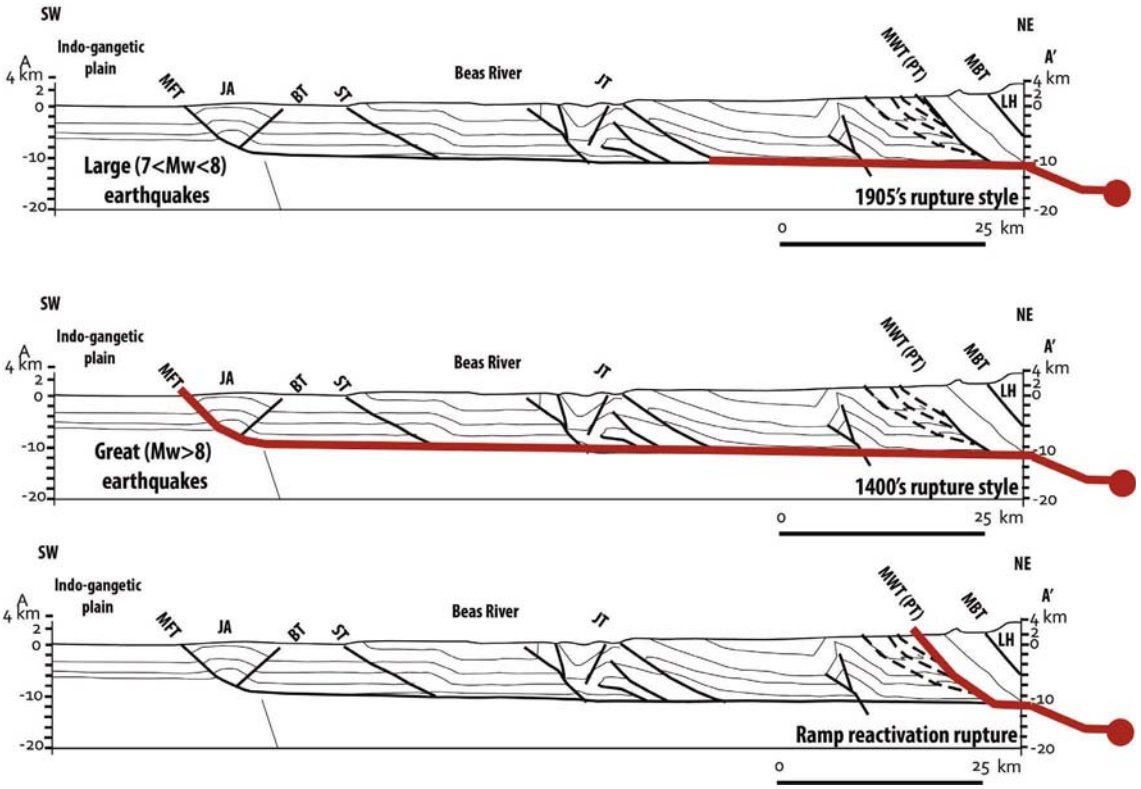

Fig. 9. Interpreted rupture styles affecting the Kangra Reentrant region. (a) 1905 rupture style, restricted to the MHT north of the Jawalamukhi Thrust; (b) Great earthquakes as the one of ~1400 A.C.; the potential reactivation of ramps as those herein reported is also suggested, as depicted by the segmented red line; (c) earthquakes nucleating at the deep MHT and propagating along ramps such as those of the PT in the study area. (b and c) Ruptures may be responsible for the scarps visible in the study area. The seismogenic downdip limit of the MHT is depicted by a red circle. Following Mugnier et al. (2013) and Seeber and Armbruster (1981).

ductile transition of the Main Himalayan Thrust and emerging at the surface along upper-crustal ramps. These earthquakes may result in a severe impact for the Kangra District, which currently hosts 1.5 million people.

Acknowledgements

We thank the positive and constructive revision made by two anonymous reviewers and the Editor Mei-Fu Zhou. This research was funded by the INSU project *Néotectonique et aléa sismique dans le Nord-Ouest Himalaya*. This work is part of the postdoctoral research of Cortés-Aranda, granted by Becas Chile. We thank Kangra Region inhabitants for their help in the fieldwork and their witness statements about earthquakes felt. Pleiades images were obtained through an ISIS project funded by the CNES. Pascal Lacroix kindly help us with image processing. We finally thank Dr. Andrew Menzies and Dr. Matt Miller for English editing.

References

Ader, T., Avouac, J.P., Liu-Zeng, J., Lyon-Caen, H., Bollinger, L., Galetzka, J., Genrich, J., Thomas, M., Chanard, K., Sapkota, S.N., Rajaure, S., Shrestha, P., Ding, L., Flouzat, M., 2012. Convergence rate across the Nepal Himalaya and interseismic coupling on the Main Himalayan Thrust: implications for seismic hazard. J. Geophys. Res. 117, B04403.

Ahmad, B., Sana, H., Alam, A., 2013. Macroseismic intensity assessment of 1885 Baramulla Earthquake of northwestern Kashmir Himalaya, using the Environmental Seismic Intensity scale (ESI 2007). Quaternary International, vol. 321, 13 February 2014, Pages 59-64, ISSN 1040-6182.

Ambraseys, N., Lensen, G., Moinfar, M., 1975. The Pattan earthquake of 28 Dec. 1974, Reconnaissance report prepared for the Government of Pakistan and UNESCO, Paris.

Ambraseys, N., Bilham, R., 2000. A note on the Kangra Ms = 7.8 earthquake of 4 April 1905. Curr. Sci. 79, 45–50.

Ambraseys, N., Douglas, J., 2004. Magnitude calibration of north Indian earthquakes. Geophys. J. Int. 159, 165–206.

Ambraseys, N., Jackson, D., 2003. A note on early earthquakes in northern India and southern Tibet. Curr. Sci. 84, 570–582.

Anderson, R.S., Repka, J.L., Dick, G.S., 1996. Explicit treatment of inheritance in dating depositional surfaces using in situ 10Be and 26Al. Geology 24, 47–51.

Arnold, M., Merchel, S., Bourlès, D.L., Braucher, R., Benedetti, L., Finkel, R.C., Aumaître, G., Gottdang, A., Klein, M., 2010. The French accelerator mass spectrometry facility ASTER: Improved performance and developments. Nucl. Instrum. Methods Phys. Res. Sect. B: Beam Interactions Mater. Atoms 268, 1954–1959.

Avouac, J.P., Ayoub, F., Leprince, S., Konca, O., Helmberger, D.V., 2006. The 2005, M w 7.6 Kashmir earthquake: sub-pixel correlation of ASTER images and seismic waveforms analysis. Earth Planet. Sci. Lett. 249, 514–528.

Balco, G., Stone, J.O., Lifton, N.A., Dunai, T.J., 2008. A complete and easily accessible means of calculating surface exposure ages or erosion rates from 10Be and 26Al measurements. Quat. Geochronol. 3, 174–195.

Banerjee, P., Burgmann, R., 2002. Convergence across the northwest Himalaya from GPS measurements. Geophys. Res. Lett. 29.

Bettinelli, P., Avouac, J.P., Flouzat, M., Jouanne, F., Bollinger, L., Willis, P., Chitrakar, G.R., 2006. Plate motion of India and interseismic strain in the Nepal Himalaya from GPS and DORIS measurements. J. Geodesy 80, 567–589.

Bevington, P.R., Robinson, D.K., 2003. Data Reduction and Error Analysis for the Physical Sciences, third ed. McGraw-Hill, MA.

Bilham, R., Wallace, K., 2006. Future Mw > 8 earthquakes in the Himalaya: implications from the 26 December 2004 Mw = 9.0 earthquake on India's eastern plate margin. Geol. Surv. Ind. Spl. Pub 85, 1–14.

Bookhagen, B., Fleitmann, D., Nishiizumi, K., Strecker, M.R., Thiede, R.C., 2006. Holocene monsoonal dynamics and fluvial terrace formation in the northwest Himalaya, India. Geology 34, 601–604.

Braucher, R., Del Castillo, P., Siame, L., Hidy, A.J., Bourlès, D.L., 2009. Determination of both exposure time and denudation rate from an in situ-produced 10Be depth profile: a mathematical proof of uniqueness. Model sensitivity and applications to natural cases. Quat. Geochronol. 4, 56–67.

Braucher, R., Merchel, S., Borgomano, J., Bourlès, D.L., 2011. Production of cosmogenic radionuclides at great depth: a multi-element approach. Earth Planet. Sci. Lett. 309, 1–9.

Burgess, W., Yin, A., Dubey, C.S., Shen, Z.K., Kelty, T.K., 2012. Holocene shortening across the main frontal thrust zone in the eastern Himalaya. Earth Planet. Sci. Lett. 357–358, 152–167.

DeCelles, P.G., Gehrels, G.E., Quade, J., Ojha, T.P., Kapp, P.A., Upreti, B.N., 1998. Neogene foreland basin deposits, erosional unroofing, and the kinematic history of the Himalayan fold-thrust belt, western Nepal. Geol. Soc. Am. Bull. 110, 2–21.

Delmas, M., Braucher, R., Gunnell, Y., Guillou, V., Calvet, M., Bourlès, D., 2015. Constraints on Pleistocene glaciofluvial terrace age and related soil chronosequence features from vertical 10Be profiles in the Ariège River catchment (Pyrenees, France). Glob. Planet. Change 132, 39–53.

DeMets, C., Calais, E., Merkouriev, S., 2017. Reconciling geodetic and geological estimates of recent plate motion across the Southwest Indian Ridge. Geophys. J. Int. 208, 118–133.

DeMets, C., Gordon, R.G., Argus, D.F., Stein, S., 1994. Effect of recent revisions to the geomagnetic reversal time scale on estimate of current plate motions. Geophys. Res. Lett. 21, 2191–2194.

DeMets, C., Gordon, R.G., Argus, D.F., Stein, S., 1990. Current plate motions. Geophys. J. Int. 101, 425–478.

Devi, R.M., Bhakuni, S.S., Bora, P.K., 2011. Neotectonic study along mountain front of northeast Himalaya, Arunachal Pradesh, India. Environ. Earth Sci. 63, 751–762.

Dey, S., Thiede, R.C., Schildgen, T.F., Wittmann, H., Bookhagen, B., Scherler, D., Strecker, M.R., 2016. Holocene internal shortening within the northwest Sub-Himalaya: out-of-sequence faulting of the Jwalamukhi Thrust, India. Tectonics 35, 1–21.

Dunne, J., Elmore, D., Muzikar, P., 1999. Scaling factors for the rates of production of cosmogenic nuclides for geometric shielding and attenuation at depth on sloped surfaces. Geomorphology 27, 3–11.

Duputel, Z., Vergne, J., Rivera, L., Wittlinger, G., Farra, V., Hetenyi, G., 2016. The 2015 Gorkha earthquake: a large event illuminating the Main Himalayan Thrust fault. Geophys. Res. Lett. 43, 2517–2525.

Gansser, A., 1983. Geology of the Bhutan Himalaya. Birkhaüser Verlag.

Gansser, A., 1964. Geology of the Himalayas, 289. InterScience Publishers.

Gavillot, Y., Meigs, A., Yule, D., Heermance, R., Rittenour, T., Madugo, C., Malik, M., 2016. Shortening rate and Holocene surface rupture on the Riasi fault system in the Kashmir Himalaya: active thrusting within the Northwest Himalayan orogenic wedge. Geol. Soc. Am. Bull. 128, 1070–1094.

Gosse, J.C., Phillips, F.M., 2001. Terrestrial in situ cosmogenic nuclides: theory and application. Quat. Sci. Rev. 20, 1475–1560.

Hidy, A.J., Gosse, J.C., Pederson, J.L., Mattern, J.P., Finkel, R.C., 2010. A geologically constrained Monte Carlo approach to modeling exposure ages from profiles of cosmogenic nuclides: an example from Lees Ferry, Arizona. Geochem., Geophys. Geosyst. 11.

Hough, S.E., Bilham, R., Ambraseys, N., Feldl, N., 2005. Revisiting the 1897 Shillong and 1905 Kangra earthquakes in northern India: site response, Moho reflections and a triggered earthquake. Curr. Sci. 88, 1632–1638.

Jackson, J., Yielding, G., 1983. The seismicity of Kohistan, Pakistan: source studies of the Hamran (1972.9.3), Darel (1981.9.12) and Patan (1974.12.28) earthquakes. Tectonophysics 91, 15–28.

Jayangondaperumal, R., Mugnier, J.L., Dubey, A.K., 2013. Earthquake slip estimation from the scarp geometry of Himalayan Frontal Thrust, western Himalaya: implications for seismic hazard assessment. Int. J. Earth Sci. 102, 1937–1955.

Joshi, M., Thakur, V.C., 2016. Signatures of 1905 Kangra and 1555 Kashmir Earthquakes in Medieval Period Temples of Chamba Region, Northwest Himalaya. Seismol. Res. Lett. 87.

Jouanne, F., Mugnier, J.L., Sapkota, S.N., Bascou, P., Pecher, A., 2017. Estimation of coupling along the Main Himalayan Thrust in the central Himalaya. J. Asian Earth Sci. 133, 62–71.

Kaneda, H., Nakata, T., Tsutsumi, H., Kondo, H., Sugito, N., Awata, Y., Akhtar, S.S., Majid, A., Khattak, W., Awan, A.A., Yeats, R.S., Hussain, A., Ashraf, M., Wesnousky, S.G., Kausar, A.B., 2008. Surface rupture of the 2005 Kashmir, Pakistan, earthquake and its active tectonic implications. Bull. Seismol. Soc. Am. 98, 521–557.

Karunakaran, C., Rao, R.A., 1979. Status of exploration for hydrocarbons in Himalayan Region – contribution to stratigraphy and structure. Misc. Pub. Geol. Sur. Ind. 41, 1–66.

Kumar, S., Wesnousky, S.G., Rockwell, T.K., Briggs, R.W., Thakur, V.C., Jayangondaperumal, R., 2005. Paleoseismic evidence of great surface rupture earthquakes along the Indian Himalaya. J. Geophys. Res. Solid Earth 111, 1–19.

Kondo, H., Nakata, T., Akhtar, S.S., Wesnousky, S.G., Sugito, N., Kaneda, H., Tsutsumi, H., Khan, A.M., Khattak, W., Kausar, A.B., 2008. Long recurrence interval of faulting beyond the 2005 Kashmir earthquake around the northwestern margin of the Indo-Asian collision zone. Geology 36, 731.

Kundu, B., Yadav, R.K., Bali, B.S., Chowdhury, S., Gahalaut, V.K., 2014. Oblique convergence and slip partitioning in the NW Himalaya: implications from GPS measurements. Tectonics 33, 2013–2024.

Lal, D., 1991. Cosmic ray labeling of erosion surfaces: in situ nuclide production rates and erosion models. Earth Planet. Sci. Lett. 104, 424–439.

Lavé, J., Avouac, J.P., 2000. Active folding of fluvial terraces across the Siwaliks Hills, Himalayas of central Nepal. J. Geophys. Res. 105, 5735.

Le Fort, P., 1975. Himalayas: the collided range. Present knowledge of the continental arc. Am. J. Sci 275, 1–44.

Lyon-Caen, H., Molnar, P., 1985. Gravity anomalies, flexure of the Indian Plate, and the structure, support and evolution of the Himalaya and Ganga Basin. Tectonics 4, 513–538.

Malik, J.N., Mohanty, C., 2007. Active tectonic influence on the evolution of drainage and landscape: geomorphic signatures from frontal and hinterland areas along the Northwestern Himalaya, India. J. Asian Earth Sci. 29, 604–618.

Malik, J.N., Nakata, T., Philip, G., Suresh, N., Virdi, N.S., 2008. Active fault and paleoseismic investigation: evidence of a historic earthquake along Chandigarh fault in the frontal Himalayan zone, NW India. Himal. Geol. 29, 109–117.

Malik, J.N., Sahoo, S., Satuluri, S., Okumura, K., 2015. Active fault and paleoseismic studies in Kangra Valley: evidence of surface rupture of a Great Himalayan 1905 Kangra Earthquake (Mw 7.8), Northwest Himalaya, India. Bull. Seismol. Soc. Am. 105, 2325–2342.

Meigs, A., Burbank, D.W., Beck, R.A., 1995. Middle-Late Miocene (pre-10 Ma) initiation of the Main Boundary Thrust in the western Himalaya. Geology 23, 423–426.

Metcalfe, R.P., 1993. Pressure, temperature and time constraints on metamorphism across the Main Central Thrust zone and High Himalayan Slab in the Garhwal Himalaya. Geol. Soc. London Spec. Publ. 74, 485–509.

Mugnier, J.-L., Huyghe, P., Chalaron, E., Mascle, G., 1994. Recent movements along the Main Boundary Thrust of the Himalayas: normal faulting in an over-critical thrust wedge? Tectonophysics 238, 199–215.

Mugnier, J.L., Leturmy, P., Huyghe, P., Chalaron, E., 1999. The Siwaliks of western Nepal II. Mechanics of the thrust wedge. J. Asian Earth Sci. 17, 643–657.

Mugnier, J.-L., Huyghe, P., Leturmy, P., Jouanne, F., 2004. Episodicity and rates of thrust sheet motion in Himalaya (western Nepal). Thrust Tectonics Hydrocarb. Syst. 82, 91–114.

Mugnier, J.L., Huyghe, P., Gajurel, A.P., Becel, D., 2005. Frontal and piggy-back seismic ruptures in the external thrust belt of Western Nepal. J. Asian Earth Sci. 25, 707–717.

Mugnier, J.L., Gajurel, A., Huyghe, P., Jayangondaperumal, R., Jouanne, F., Upreti, B., 2013. Structural interpretation of the great earthquakes of the last millennium in the central Himalaya. Earth-Sci. Rev. 127, 30–47.

Mugnier, J.L., Vignon, V., Jayangondaperumal, R., Vassallo, R., Malik, M.A., Replumaz, A., Srivastava, R.P., Jouanne, F., Buoncristiani, J.F., Jomard, H., Carcaillet, J., 2017. A complex thrust sequence in western Himalaya: the active Medlicott Wadia Thrust. Quat. Int. 462, 109–123.

Mukherjee, S., 2015. A review on out-of-sequence deformation in the Himalaya. Geol. Soc. London, Spec. Publ. 412, SP412-SP413.

Murphy, M.A., Taylor, M.H., Gosse, J., Silver, C.R.P., Whipp, D.M., Beaumont, C., 2014. Limit of strain partitioning in the Himalaya marked by large earthquakes in western Nepal. Nat. Geosci. 7, 38–42.

Owen, L.A., Caffee, M.W., Bovard, K.R., Finkel, R.C., Sharma, M.C., 2006. Terrestrial cosmogenic nuclide surface exposure dating of the oldest glacial successions in the Himalayan orogen: Ladakh Range, northern India. Geol. Soc. Am. Bull. 118, 383–392.

Parameswaran, R.M., Natarajan, T., Rajendran, K., Rajendran, C.P., Mallick, R., Wood, M., Lekhak, H.C., 2015. Seismotectonics of the April-May 2015 Nepal earthquakes: an assessment based on the aftershock patterns, surface effects and deformational characteristics. J. Asian Earth Sci. 111, 161–174.

Patriat, P., Achache, J., 1984. India-Eurasia collision chronology has implications for crustal shortening and driving mechanism of plates. Nature 311, 615–621.

Peltzer, G., Saucier, F., 1996. Present-day kinematics of Asia derived from geologic fault rates. J. Geophys. Res. Solid Earth 101, 27943–27956.
Powers, P.M., Lillie, R.J., Yeats, R.S., 1998. Structure and shortening of the Kangra and Dehra Dun reentrants, Sub-Himalaya, India. Geol. Soc. Am. Bull. 110, 1010–1027.
Rabus, B., Eineder, M., Roth, A., Bamler, R., 2003. The shuttle radar topography mission—a new class of digital elevation models acquired by spaceborne radar. ISPRS J. Photogramm. Remote Sens. 57, 241–262.
Rajendran, C.P., Rajendran, K., 2005. The status of central seismic gap: a perspective based on the spatial and temporal aspects of the large Himalayan earthquakes. Tectonophysics 395, 19–39.
Ruszkiczay-Rüdiger, Z., Braucher, R., Novothny, Á., Csillag, G., Fodor, L., Molnár, G., Madarász, B., 2016. Tectonic and climatic control on terrace formation: Coupling in situ produced 10Be depth profiles and luminescence approach, Danube River, Hungary, Central Europe. Quat. Sci. Rev. 131, 127–147.
Sapkota, S.N., Bollinger, L., Klinger, Y., Tapponnier, P., Gaudemer, Y., Tiwari, D., 2013. Primary surface ruptures of the great Himalayan earthquakes in 1934 and 1255. Nat. Publ. Gr. 6, 152.
Seeber, L., Armbruster, J.G., 1981. Great detachment earthquakes along the Himalayan Arc and long-term forecasting. Am. Geophys. Union 259–277.
Seeber, L., Armbruster, J.G., Quittmeyer, R.C., 1981. Seismicity and continental subduction in the Himalayan arc. Zagros Hindu Kush Himalaya Geodyn. Evol. 215–242.
Stone, J.O., 2000. Air pressure and cosmogenic isotope production. J. Geophys. Res. Solid Earth 105, 23753–23759.
Szeliga, W., Bilham, R., 2017. New constraints on the mechanism and rupture area for the 1905 Mw 7.8 kangra earthquake, northwest himalaya: new constraints on the mechanism and rupture area for the 1905 Mw 7.8 kangra earthquake. Bull. Seismol. Soc. Am. 107, 2467–2479.
Thakur, V.C., Jayangondaperumal, R., Malik, M.A., 2010. Redefining Medlicott-Wadia's main boundary fault from Jhelum to Yamuna: an active fault strand of the main boundary thrust in northwest Himalaya. Tectonophysics 489, 29–42.
Thakur, V.C., Joshi, M., Sahoo, D., Suresh, N., Jayangondapermal, R., Singh, A., 2014. Partitioning of convergence in Northwest Sub-Himalaya: estimation of late quaternary uplift and convergence rates across the Kangra reentrant, North India. Int. J. Earth Sci. 103, 1037–1056.
Vassallo, R., Mugnier, J.-L., Vignon, V., Malik, M.A., Jayangondaperumal, R., Srivastava, P., Jouanne, F., Carcaillet, J., 2015. Distribution of the Late-Quaternary deformation in Northwestern Himalaya. Earth Planet. Sci. Lett. 411, 241–252.
Vignon, V., Mugnier, J.L., Vassallo, R., Srivastava, P., Malik, M.A., Jayangondaperumal, R., Jouanne, F., Buoncristiani, J.F., Carcaillet, J., Replumaz, A., Jomard, H., 2017. Sedimentation close to the active Medlicott Wadia Thrust (Western Himalaya): how to estimate climatic base level changes and tectonics. Geomorphology 284, 175–190.
Wallace, K., Bilham, R., Blume, F., Gaur, V.K., Gahalaut, V., 2005. Surface deformation in the region of the 1905 Kangra Mw = 7.8 earthquake in the period 1846–2001. Geophys. Res. Lett. 32, 1–5.
Wesnousky, S.G., Kumar, S., Mohindra, R., Thakur, V.C., 1999. Uplift and convergence along the Himalaya Frontal Thrust of India. Tectonics 18, 967–976.
Wobus, C.W., Whipple, K.X., Hodges, K.V., 2006. Neotectonics of the central Nepalese Himalaya: constraints from geomorphology, detrital40Ar/39Ar thermochronology, and thermal modeling. Tectonics 25, 1–18.
Yin, A., 2006. Cenozoic tectonic evolution of the Himalayan orogen as constrained by along-strike variation of structural geometry, exhumation history, and foreland sedimentation. Earth-Sci. Rev. 76, 1–131.
Zhao, W., Nelson, K.D., Che, J., Quo, J., Lu, D., Wu, C., Liu, X., 1993. Deep seismic reflection evidence for continental underthrusting beneath southern Tibet. Nature 366, 557–559.